

Lawrence Berkeley National Laboratory

Lawrence Berkeley National Laboratory

Title

RESULTS ON CHARMED BARYONS AND MESONS FROM THE SLAC-LBL
MARK II DETECTOR AT SPEAR

Permalink

<https://escholarship.org/uc/item/4b03p4q1>

Author

Goldhaber, G.

Publication Date

1980

Peer reviewed

Talk presented at the Topical Workshop
on the Production of New Particles in
Supe: High Energy Collisions, University
of Wisconsin, Madison, WI; October 22-24,
1979.

LBL-10428

RESULTS ON CHARMED BARYONS AND MESONS
FROM THE SLAC-LBL MARK II DETECTOR AT SPEAR

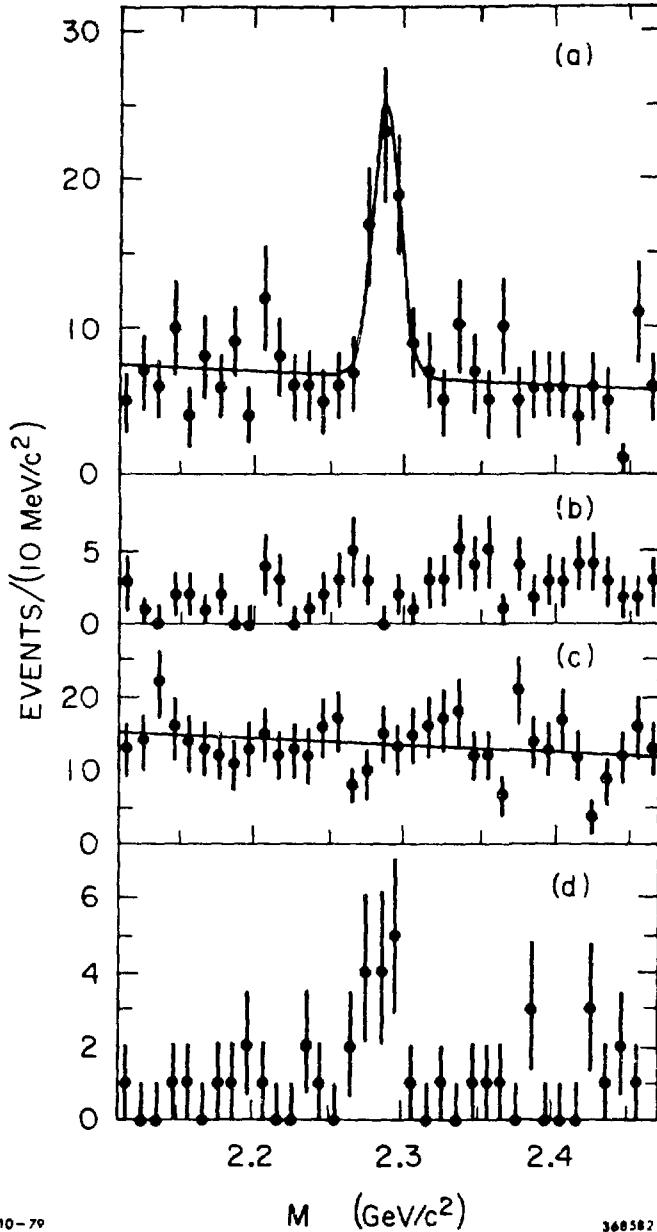
Gerson Goldhaber
Department of Physics and Lawrence Berkeley Laboratory
University of California, Berkeley, California 94720

In my talk I will present results from the SLAC-LBL Mark II detector at SPEAR. Our detector has been described elsewhere¹ and I will not discuss it here. I will concentrate here on a few of the very recent results, namely:

- (1) The observation of charmed baryons; we have now clearly established a signal $\Lambda_c \rightarrow p\bar{K}^-\pi^+$ and the charge conjugate of that channel, $\bar{\Lambda}_c \rightarrow \bar{p}K^+\pi^-$. We also have some evidence for other channels, $K_S^0 p$, $\Lambda\pi^+$, etc.
- (2) The study of charmed mesons. Here I will mention some new hadronic decay modes, and the Cabibbo-suppressed decay modes.
- (3) The D^+ - D^0 lifetime ratio; we find evidence that the D^+ has a longer lifetime than the D^0 by about a factor of three, although the statistical error is fairly large on this number.

(1) Observation of the Charmed Baryon in e^+e^- Annihilation

Our present understanding of the charmonium states and of charmed mesons leads us to expect the existence of weakly decaying charmed baryons.² Evidence for the production of such charmed baryons has been reported in neutrino interactions,³ photon interactions,⁴ and p-p interactions.⁵ The signal we have observed for charmed baryon production is given in Fig. 1a. Here we see a peak of about 39 ± 8 events over a background level of 20 events. The peak occurs in the $p\bar{K}^-\pi^+$ and in the charge conjugate system. Furthermore in this figure we have made a recoil cut, demanding that the recoil mass be greater than 2.2 GeV. In Fig. 1b we show what happens when you look at the same mass distribution with a recoil mass cut less than 2.2 GeV. We thus see that the signal we have observed is associated with the production of an equal or larger mass. In Fig. 1c we show the mass distributions for combinations which either have the wrong strangeness, namely $pK^+\pi^-$, a positively charged baryon, but with positive strangeness and $p\bar{K}^-\pi^-$ which is a negatively charged baryon with negative strangeness (and their charge conjugate states). Neither



10-79

368582

Fig. 1. The combined $pK^-\pi^+$ and $\bar{p}K^+\pi^-$ mass distribution (a) for recoil masses greater than $2.2 \text{ GeV}/c^2$, and (b) for recoil masses less than $2.2 \text{ GeV}/c^2$. (c) The $pK^+\pi^-$ and $pK^-\pi^-$ (and charge conjugate states) mass distribution for recoil masses greater than $2.2 \text{ GeV}/c^2$. (d) The beam-constrained mass distribution for events with $pK^-\pi^+$ or $\bar{p}K^+\pi^-$ energy within 0.03 GeV of the beam energy.

of these are expected to occur as the final states from charmed baryon decay, and indeed we see no signal. The curve through Fig. 1c (suitably normalized) is used as the background for Fig. 1a. Finally in Fig. 1d we give the beam-energy-constrained mass M_C . This was obtained by making a cut on the total energy of the $pK\pi$ system, by demanding that it be within 30 MeV of the beam energy. We then calculate M_C from $M_C = (E_b^2 - p_{pK\pi}^2)^{1/2}$ and we find that there is an equal mass signal. The signal is small, but it is clear cut and consists of 10 ± 4 events. This corresponds to $\Lambda_c \bar{\Lambda}_c$ production and we estimate $(26 \pm 11)\%$ of the total Λ_c production for this process. Figure 2 shows the $pK\pi$ mass distribution now separated into $pK^-\pi^+$ and $\bar{p}K^+\pi^-$. The figure is given in 20-MeV bins and again we see that the signal clearly occurs in both systems. The background due to beam gas scattering is larger for proton events than for antiproton events. In Fig. 1 we have made cuts to reduce the amount of beam gas background. This was done by cutting out events where the total positive charge was greater than one. This selection was not made in Fig. 2. The sample we have studied corresponds to $9,150 \text{ nb}^{-1}$ in the energy region $E_{C,m.} = 4.5 - 6 \text{ GeV}$. Of this data, nearly half was taken at the single energy of $E_{C,m.} = 5.2 \text{ GeV}$. The data-taking at 5.2 GeV was carried out in the last three weeks of the running at SPEAR. The Mark II detector has now been moved to PEP and is located in Interaction Region 12. Thus it was these last three weeks of running at SPEAR which gave us most of the clear signal that we see here!

.The Mass Measurement. The protons and K's were identified by time-of-flight measurements. The rms width of the TOF measurements, σ , is 0.3 ns. This gives us a 1σ separation between K's and p's up to 2 GeV, and a corresponding separation for K's and π 's up to 1.35 GeV. We found a mass value of $2.285 \pm 0.006 \text{ GeV}$ with an rms energy resolution of 10 MeV. The Λ_c mass measurement is based on two results. One is the direct invariant mass distribution. Here we have the full statistics and get a mass of 2286 MeV with an error of 7 MeV. In this case the statistical error is small and a 6-MeV systematic error is the main contributor. We also get an independent measurement from the beam-constrained mass. Here we find a mass of 2284. This time, however, the statistical error is much larger, giving a total error of 8 MeV. It is interesting to note that an error in momentum affects these two results in opposite directions; we thus have a confirmation that our momentum measurement is self-consistent.

This result is somewhat surprising since the earlier indications for

$M_{RECOL} > 2.2 \text{ GeV}$

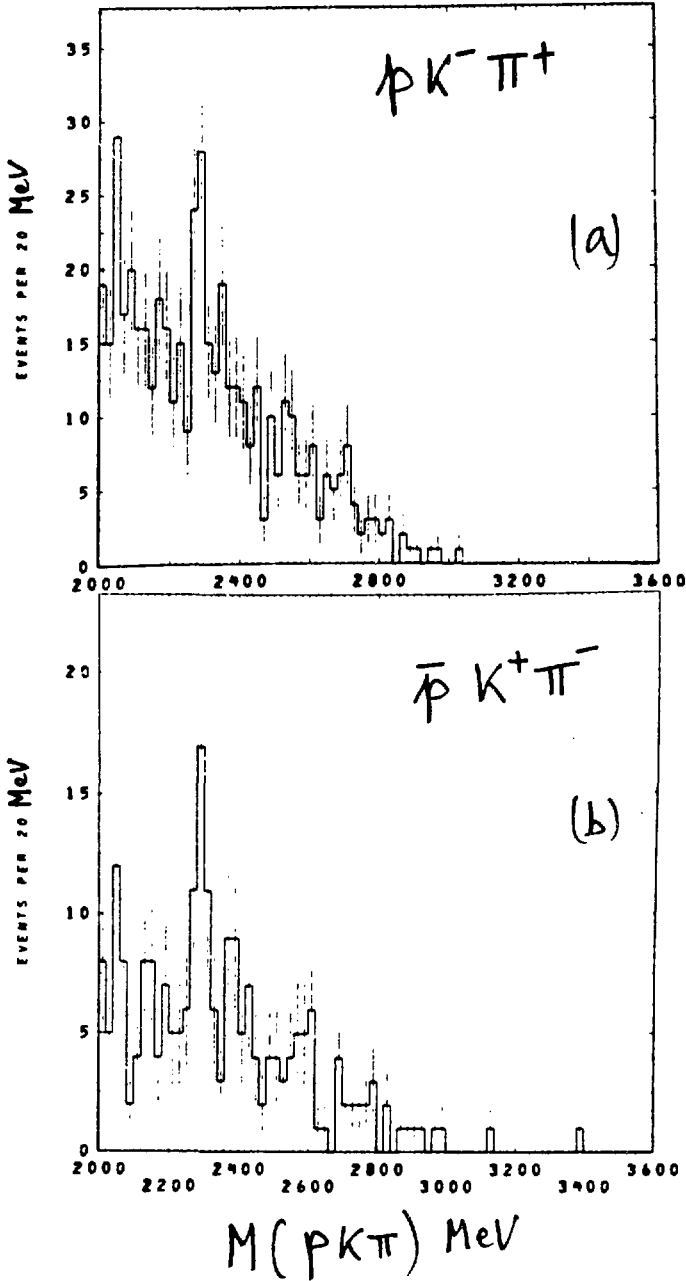


Fig. 2. Invariant mass of $pK^-\pi^+$ system and $\bar{p}K^+\pi^-$ systems.

charmed baryons appeared to be 25-30 MeV lower in mass.^{3,4,5} This raises the question: how well can we measure effective masses in our device? The answer is that we find excellent agreement with established mass values in the measurement of well-known states. To convince you of our ability to measure masses in the Mark II detector, I will now show you a few examples of well-established masses which we have measured. In Fig. 3a we show 20,000 K^0 's obtained at the J/ψ . We find a mass of 498.0 MeV to be compared with the "world average" value of 497.7 MeV. In Fig. 3b we have the ψ itself going into μ pairs; we find a mass of 3.0967 GeV, to be compared with 3.095 GeV which is the energy scale calibration we established at SPEAR during running with the SLAC-LBL Mark I detector. The difference is of course that in Fig. 3b is the measured invariant mass which depends purely on measurements in the Mark II detector and is independent of the beam energy. In Fig. 4a I show a measurement of the $\Lambda\pi^-$ mass corresponding to the reaction: $\psi \rightarrow \Xi + \text{anything}$. We find the Ξ mass as 1320 MeV, which is within 1 MeV of the "world average" value of 1321.3 MeV. This reaction at the ψ giving cascade hyperons corresponds largely to $\psi \rightarrow \Xi\Xi^-$ and Fig. 4b shows the beam-constrained mass, which as I stated above depends on the measured momenta in the opposite way from the invariant mass. Here too we find a mass value within 1 MeV of the other case. Figure 4c shows the recoil mass spectrum against the Ξ and we see that the reaction is primarily $\psi \rightarrow \Xi\Xi^-$ with a small contribution of $\psi \rightarrow \Xi\Xi^*(1530)$.

Two-Body Structure in the $pK\pi$ System. An analysis of the Λ_c Dalitz plot yields estimates of resonant contributions to the observed Λ_c signal of $12 \pm 7\%$ $17 \pm 7\%$ for the $K^{*0}(890) \rightarrow K^- \pi^+$ and $\Delta^{++}(1230)$, respectively. Figure 5 gives the corresponding mass projections. The pK^- projection, not given here, shows no evidence for any Y^* structure.

Cross-Section Determination (σ_B). To determine a cross section, the detection efficiency has been calculated to be 0.13 ± 0.025 for the observed Λ_c momentum distribution. The 26 ± 7 $pK\pi$ signal events observed in the 5450-nb^{-1} integrated luminosity within 0.05 GeV of 5.2-GeV c.m. energy correspond to

$$\sigma(\Lambda_c + \bar{\Lambda}_c)B(\Lambda_c \rightarrow pK^- \pi^+) = 0.037 \pm 0.012 \text{ nb},$$

where $\sigma(\Lambda_c + \bar{\Lambda}_c)$ is defined as the inclusive cross section [$\sigma(\Lambda_c) + \sigma(\bar{\Lambda}_c)$]. The data are consistent with equal cross sections for both charge states.

Inclusive p and Λ Production Rates. To obtain an estimate of the total production of charmed baryons we have measured the inclusive cross sections for

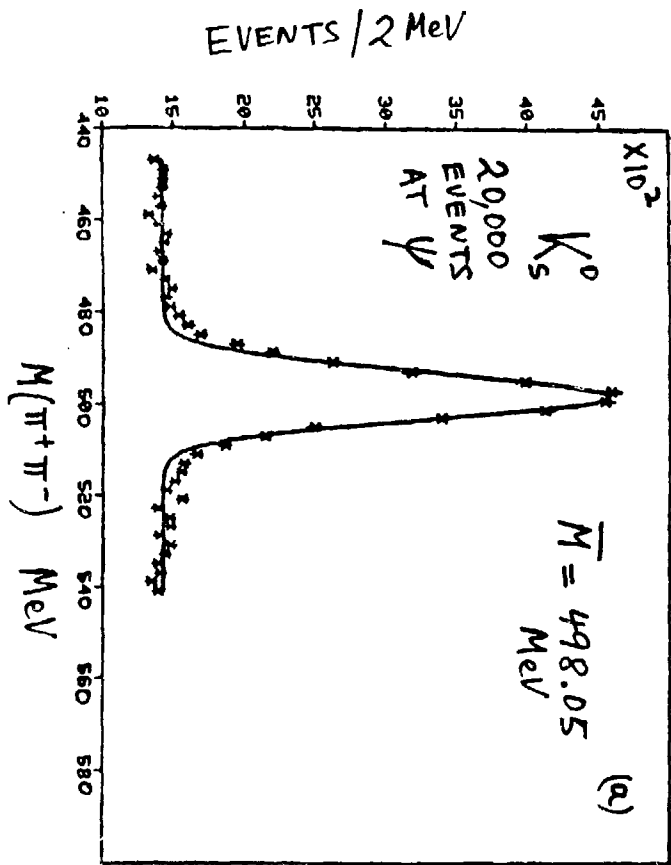
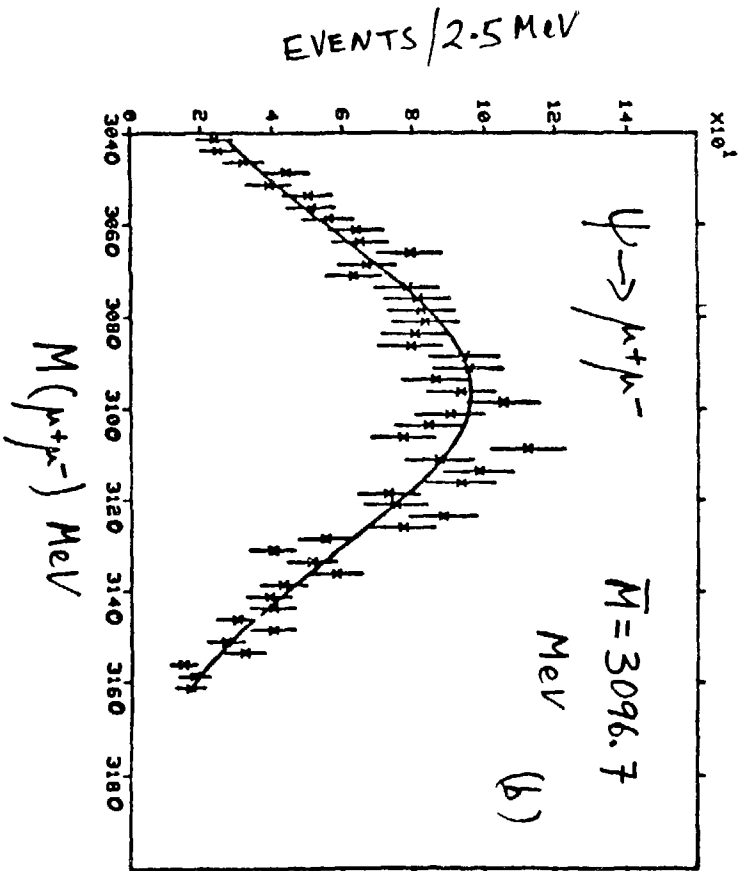


Fig. 3. Invariant masses for $\pi^+ \pi^-$ and $\mu^+ \mu^-$ systems at ψ , to illustrate absolute mass measurements in the Mark II detector.

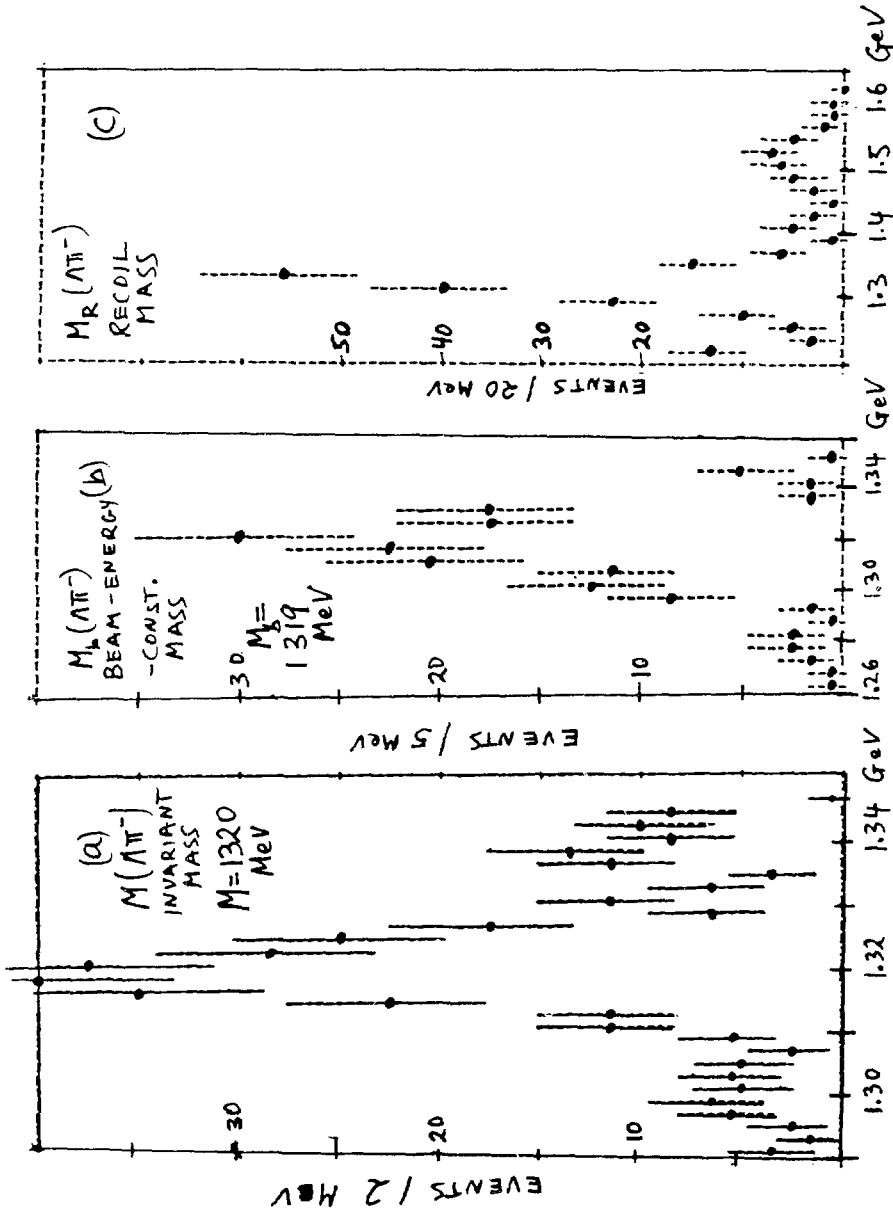


Fig. 4. Observation of $\psi \rightarrow \pi\pi^-\pi^+$ as illustration for absolute mass measurements. (a) Invariant mass of $\pi\pi^-$ ($\pi\pi^+$) system in 2-MeV bins. (b) Beam-energy-constrained mass against π in 5-MeV bins. (c) Recoil mass against π in 20-MeV bins.

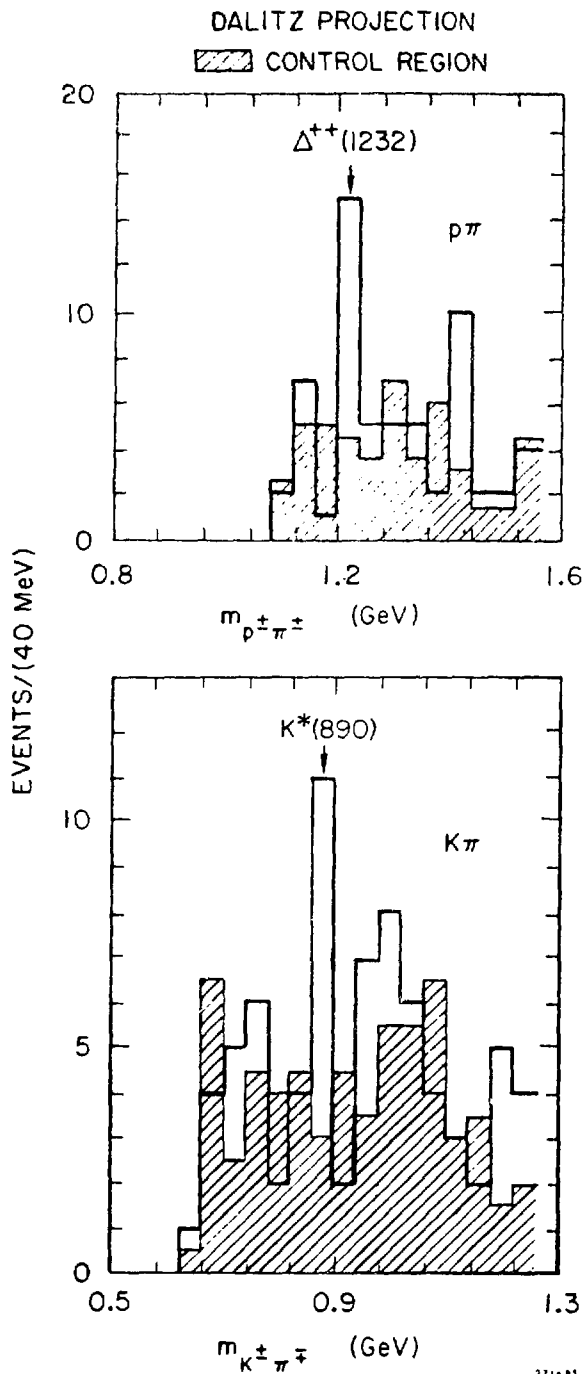


Fig. 5. Two-body masses for events in Λ_c peak.

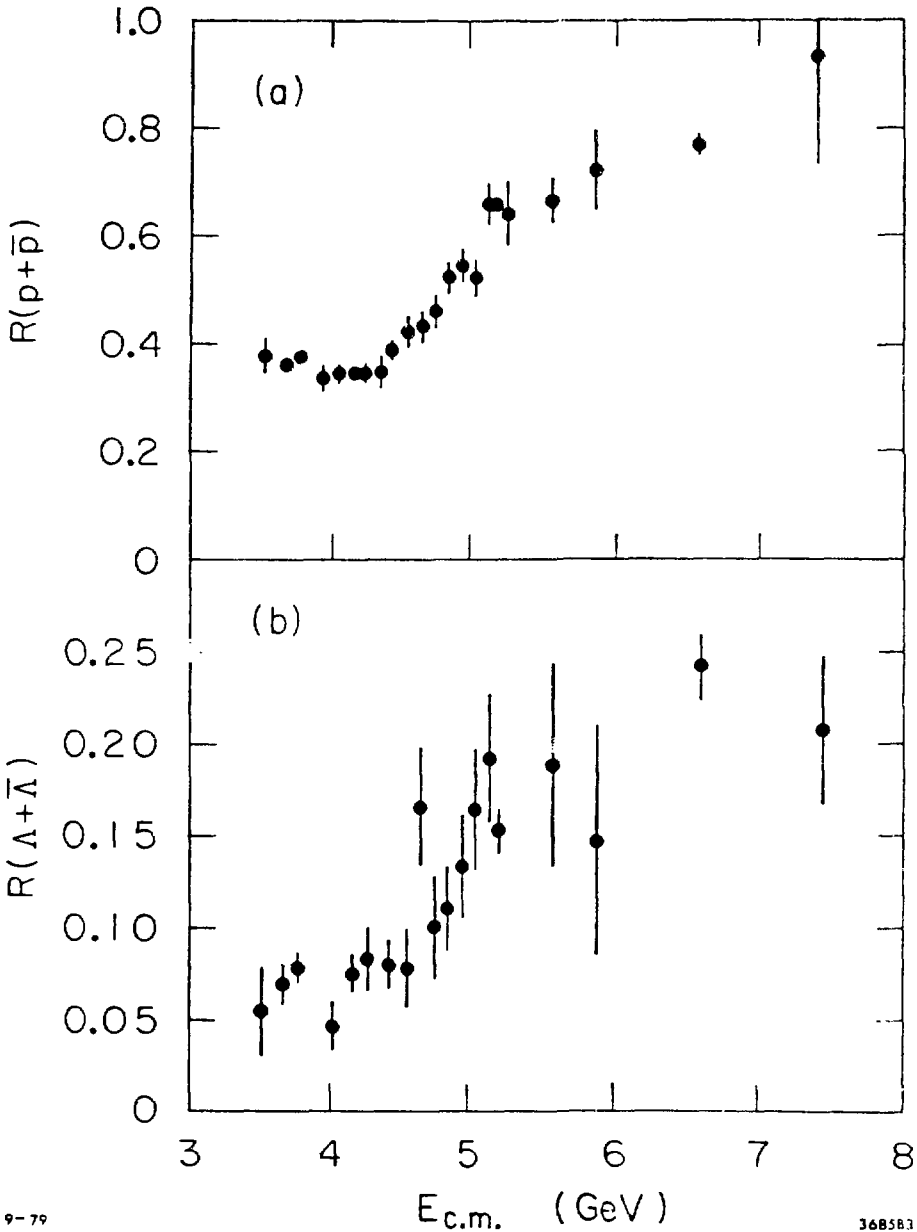
p and Λ from 3.52 to 7.40 GeV. Because of substantial beam-gas contamination in proton events, only antiprotons are used for these measurements. Two or more observed tracks are required and valid identification of antiprotons is ensured by a stricter TOF weight cut of 0.7 for momenta greater than 1.2 GeV/c. The observed p sample includes contributions from weakly decaying hyperons. For Λ and $\bar{\Lambda}$ production, only multihadron events with three or more detected tracks are used. The Λ and $\bar{\Lambda}$ are identified from the invariant-mass distribution of all neutral $p\pi$ pairs identified by TOF. In addition, the decay products of the Λ and $\bar{\Lambda}$ are required to originate from a secondary vertex. To reduce beam-gas contamination to less than 4%, Λ (but not $\bar{\Lambda}$) events are required to have total observed charge $< +1$. With these cuts, our Λ and $\bar{\Lambda}$ background subtractions are both $\lesssim 15\%$ at all energies.

The efficiency for detection of antiprotons is calculated from a Monte Carlo model which generates \bar{p} tracks with a momentum distribution corresponding to an invariant cross section

$$E \frac{d^3\sigma}{dp^3} \propto e^{-bE} ,$$

and which then chooses the other nucleon and a number of pions according to the remaining phase space. After adjustment of the slope parameter b and the mean particle multiplicity at each energy, this form gives a good description of the data. The overall detection efficiency for antiprotons is approximately 58% over the entire range 3.7-7.4 GeV. The efficiency for Λ and $\bar{\Lambda}$ detection is determined by the same Monte Carlo model with the parameters obtained from the antiprotons. The efficiency ranges from 10% at 3.67 GeV to 13% at 7.4 GeV, including the branching ratio for $\Lambda \rightarrow p\pi^-$. In this case also, the Monte Carlo calculation reproduces the observed Λ momentum and multiplicity distributions. As an additional check on our Λ efficiency calculations, we have verified that the ratio of single Λ 's and $\Lambda\bar{\Lambda}$ pairs detected in well-identified $\psi \rightarrow \Lambda\bar{\Lambda}$ events at $E_{c.m.} = 3.095$ GeV is correctly reproduced by the Monte Carlo simulation program.

Our results for inclusive production of p and Λ are presented in Fig. 6 as the ratio of the inclusive production cross section to the μ -pair cross section. Figure 6a shows $R(p + \bar{p}) \equiv 2\sigma(\bar{p})/\sigma_{\mu\mu}$ and Fig. 6b shows $R(\Lambda + \bar{\Lambda}) \equiv [\sigma(\Lambda) + \sigma(\bar{\Lambda})]/\sigma_{\mu\mu}$. The estimated overall systematic errors in R are $\pm 17\%$ and $\pm 27\%$ for the p and Λ , respectively, and are not shown in Fig. 6. These systematic errors are dominated by the model dependence of the Monte Carlo calculations, and are expected to vary slowly over our energy region.



9-79

368581

Fig. 6. (a) $R(p + \bar{p})$ as a function of $E_{c.m.}$. (b) $R(\Lambda + \bar{\Lambda})$ as a function of $E_{c.m.}$. Errors are statistical only.

We note that the rise previously reported⁶ in $R(p + \bar{p})$ and $R(\Lambda + \bar{\Lambda})$ is confirmed here with more precision. We observe for the first time clear steps in both $R(p + \bar{p})$ and $R(\Lambda + \bar{\Lambda})$ in the range of 4.5 to 5.2 GeV c.m. energy, although the R values probably continue to rise more slowly at higher energies. Within the quoted errors, our measurements of $R(p + \bar{p})$ are consistent with previous experiment,^{6,7} Our values of $R(\Lambda + \bar{\Lambda})$ are considerably higher than the previous measurements⁶ but have been obtained with larger solid angle, improved vertex reconstruction, and a more sophisticated efficiency calculation.

Branching Ratio Determination. The coincidence of the location of this step with the threshold for production of an object near the mass of the observed $pK\pi$ signal is consistent with its interpretation as the lowest-lying charmed baryon. The observed step sizes of $\Delta R(p + \bar{p}) = 0.31 \pm 0.06$ and $\Delta R(\Lambda + \bar{\Lambda}) = 0.10 \pm 0.03$ would indicate a Λ/p ratio for charmed-baryon decays of $(41 \pm 15)\%$ after explicitly removing protons which arise from Λ decay, but not from other weakly decaying strange baryons.

We can use our measurement of $R(p + \bar{p})$ and the measured σ_B for the $pK\pi$ signal at 5.2 GeV to estimate the absolute branching ratio for the $pK\pi$ decay mode. We make the following assumptions: (i) The observed step in $R(p + \bar{p})$ is due entirely to the onset of charmed-baryon pair production; (ii) all charmed baryons cascade down to the Λ_c state; and (iii) the probability for a charmed baryon to give a proton (as opposed to a neutron) as a final product is 0.6 ± 0.1 .⁸ Using the relationship

$$\sigma(\Lambda_c + \bar{\Lambda}_c) = \frac{\Delta R(p + \bar{p})}{0.6} \sigma_{\mu\mu} ,$$

we find an inclusive cross section

$$\sigma(\Lambda_c + \bar{\Lambda}_c) = 1.7 \pm 0.4 \text{ nb}$$

at 5.2 GeV. Thus the cross section for producing pairs of charmed baryons is 0.85 nb. With these assumptions, the branching ratio is then estimated to be

$$B(\Lambda_c \rightarrow pK^-\pi^+) = (2.2 \pm 1.0)\% .$$

Search for Other Decay Modes. We have looked at the channels pK_S^0 , $\Lambda\pi^+$, and $\Lambda\pi^+\pi^-\pi^+$ for additional decay modes of the Λ_c .

Figure 7b shows the pK_S^0 mass distribution compared to the $pK^-\pi^+$ distribution as in Fig. 1a. Figure 8 shows the beam-energy-constrained mass distribution for the $pK\pi$, pK_S^0 , $\Lambda\pi$ and $\Lambda 3\pi$ modes. Some evidence for the $\Lambda_c \bar{\Lambda}_c$ channel

$$M_{\text{RECOIL}} > 2.2 \text{ GeV}$$

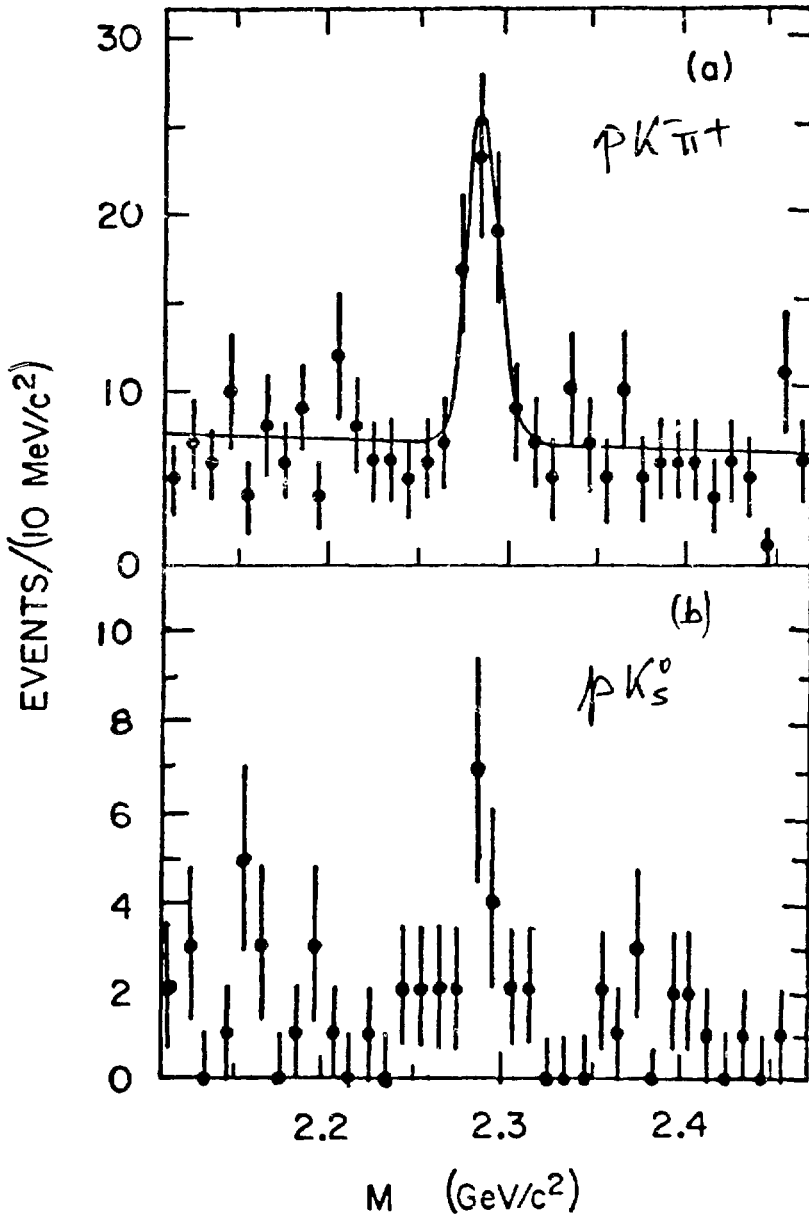


Fig. 7. (a) Repeat of Fig. 1(a), the $pK^-\pi^+$ ($\bar{p}K^+\pi^-$) invariant mass distribution. (b) The pK_S^0 invariant mass distribution.

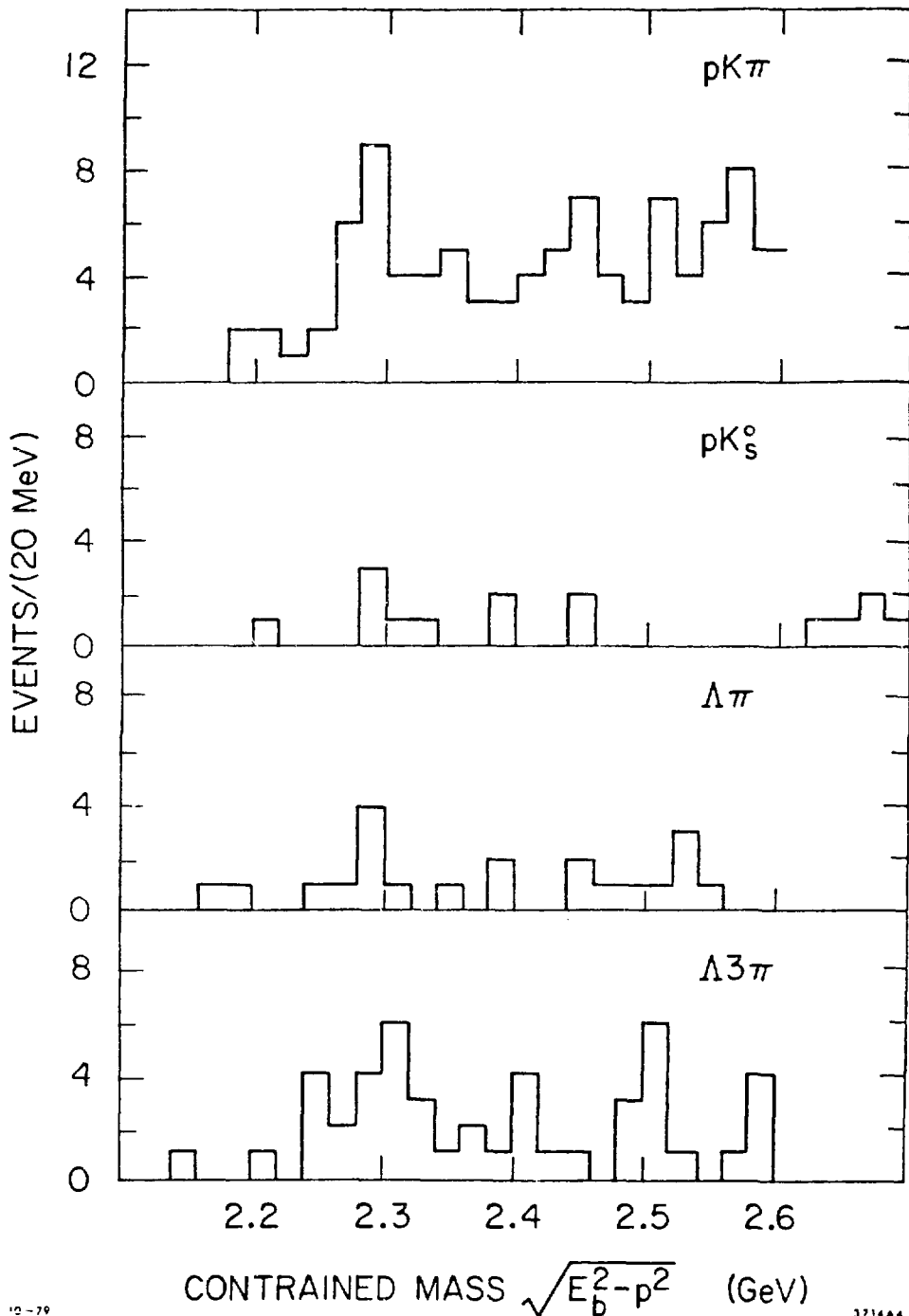


Fig. 8. Beam-energy-constrained mass distributions.

may be noted. Figure 9 shows the sum of these beam-energy-constrained distributions. Our preliminary result on these additional channels is:

$$\underline{pK_S^0}: \quad 12.5 \pm 4.5 \text{ events signal which gives } B(\Lambda_c \rightarrow p\bar{K}^0)/B(\Lambda_c \rightarrow p\bar{K}^-\pi^+) = 0.5 \pm 0.25, \text{ while we get upper limits from the beam-energy-constrained data}$$

$$\underline{\Lambda\pi^+}: \quad B(\Lambda_c \rightarrow \Lambda\pi)/B(\Lambda_c \rightarrow p\bar{K}^-\pi^+) \leq 0.6 \text{ (90\% confidence level),}$$

$$\underline{\Lambda(3\pi)^+}: \quad B(\Lambda_c \rightarrow \Lambda\pi^+\pi^+\pi^-)/B(\Lambda_c \rightarrow p\bar{K}^-\pi^+) \leq 1.4 \text{ (90\% confidence level).}$$

Conclusion on Λ_c . In conclusion, our observation of a narrow state with the proper quantum numbers, associated with equal and higher recoil masses, and at a mass compatible with the observed threshold in p and Λ production, argues for the interpretation of this state as the charmed baryon Λ_c .

(2) Charmed Meson Studies

The first observation of the charmed mesons⁹ D^0 and D^+ in the SLAC-LBL Mark I detector was made in the $E_{c.m.} = 3.9$ to 4.6 GeV region. In this energy region, and particularly at the cross-section peak at 4.028 GeV, the principal D production processes are

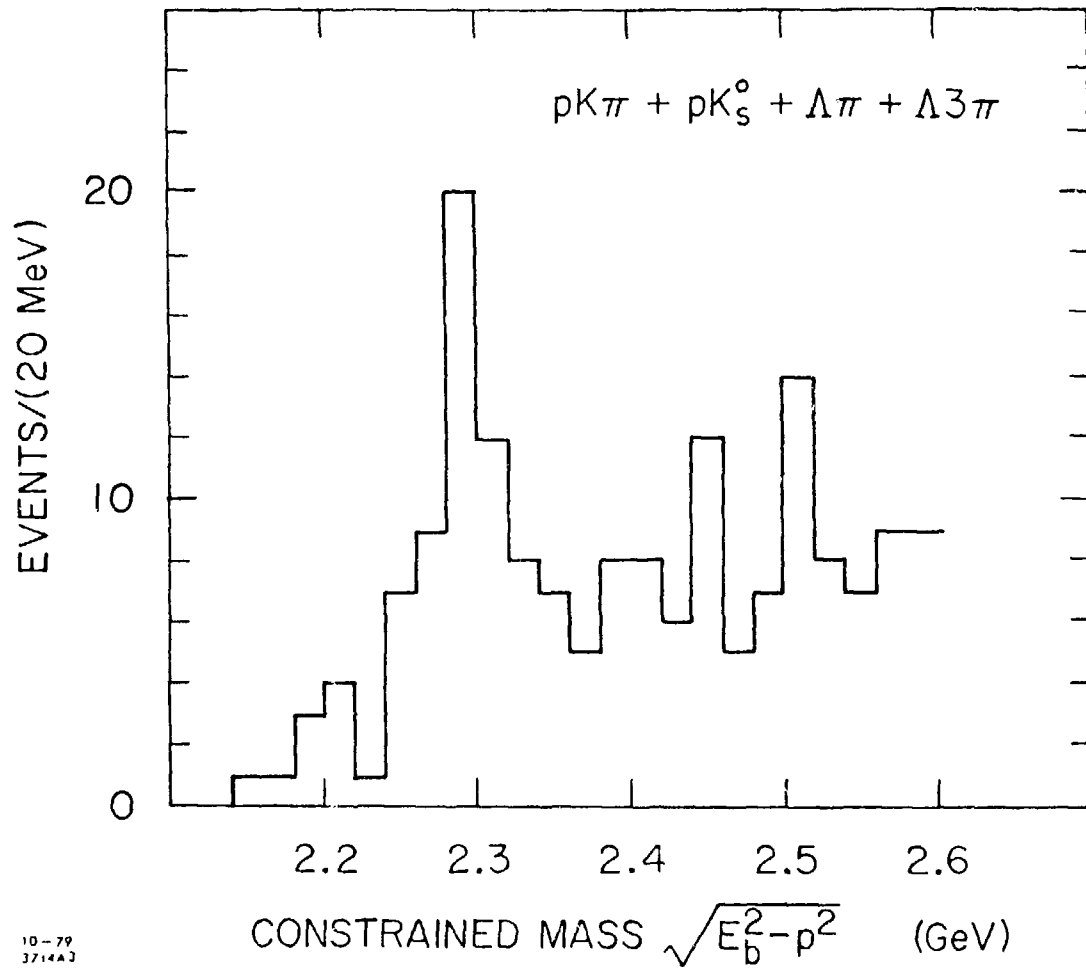
$$e^+e^- \rightarrow D^*\bar{D} \text{ or } D\bar{D}^*$$

and

$$e^+e^- \rightarrow D^*\bar{D}^*.$$

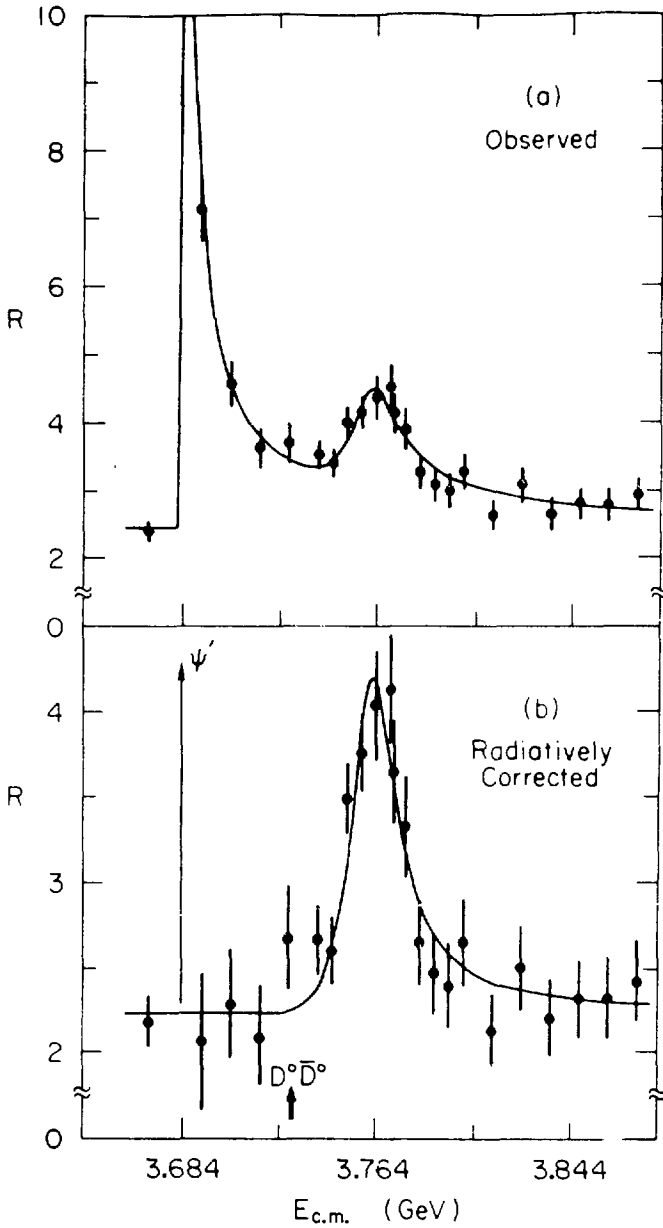
It was only at a later stage that the $\psi(3770)$ or ψ'' resonance was discovered in the LGW and DELCO experiments.^{10,11} The mass value of the ψ'' lies below the threshold for the above processes. Thus only the production of $D\bar{D}$ occurs. Namely: $e^+e^- \rightarrow \psi'' \rightarrow D^0\bar{D}^0$ and $D^+\bar{D}^-$. Thus the ψ'' which lies ~ 40 MeV above $D^0\bar{D}^0$ and ~ 30 MeV above $D^+\bar{D}^-$ threshold is ideally suited for the study of D meson properties. If we compare the width of the $\psi(3684)$ or ψ' , $\Gamma = 0.228$ MeV, with that of the ψ'' , $\Gamma = 25$ MeV, we note the width has increased by a factor of ~ 100 and thus that the effect of the OZI suppression at the ψ' is no longer present at the ψ'' . This is ascribed to the fact that the D production threshold opens up at 3726 MeV (3736 MeV for $D^+\bar{D}^-$), and hence channels with c and \bar{c} quarks in the final state can occur at the ψ'' .

Properties of the $\psi(3770)$ Resonance. The ψ'' has been studied extensively in the LGW and DELCO experiments and recently again in the SLAC-LBL Mark II experiments as I will report here. Figure 10 shows the R distribution observed in the Mark II experiment. Here R is the ratio of the hadronic cross section to the theoretical QED μ pair cross section $\sigma_{\mu\mu}$. The latter is obtained from calibration against observed Bhabha pairs. The $\tau^+\tau^-$ cross section has been



10-79
3714A2

Fig. 9. Sum of beam-energy-constrained mass distribution in Fig. 8.



XBL 801-7877

Fig. 10. (a) The data as observed is plotted in units of R . A radiative correction for the continuum ($\sim 9\%$) has been applied. Full radiative corrections are applied in (b). The curve is the fit to the data.

subtracted. Figure 10a gives this corrected value. Figure 10b gives the R distribution after the radiative tails from the J/ψ and ψ' have been subtracted. The errors shown are statistical. The resonance is fitted to a p-wave Breit-Wigner expression¹² with an energy-dependent total width $\Gamma_{\text{tot}}(E_{\text{c.m.}})$ which takes account of the vicinity of the $D^0\bar{D}^0$ and D^+D^- thresholds. Each charmed meson pair is assumed to rise from threshold in a manner characteristic of p-wave production. Here

$$R(E_{\text{c.m.}}) = \frac{1}{\sigma_{\mu\mu}} \frac{3\pi}{M^2} \frac{\Gamma_{ee} \Gamma_{\text{tot}}(E_{\text{c.m.}})}{(E_{\text{c.m.}} - M)^2 + \Gamma_{\text{tot}}^2(E_{\text{c.m.}})/4}$$

and

$$\Gamma_{\text{tot}}(E_{\text{c.m.}}) \propto \frac{p_+^3}{1 + (rp_+)^2} + \frac{p_0^3}{1 + (rp_0)^2}$$

where p_+ (p_0) is the momentum of the pair produced D^+ (D^0) and r is the interaction length. The quantities M (the resonance mass) and Γ_{ee} (the partial width to electrons) were determined in a fit to the data points. The fit is not sensitive to r which was taken as 2.5 Fermi.

The new results are consistent with the earlier data from the LGW¹³ and DELCO, except for a shift in the central mass value which is now found to be 3764 ± 5 MeV, that is 6-8 MeV lower than the previous values. A more precise measurement is ΔM , the $\psi'' - \psi'$ mass difference which does not include the systematic error of the absolute beam energy calibration. This is found to be $\Delta M = 80 \pm 2$ MeV. Furthermore the Mark II value for the width of decay into e^+e^- , $\Gamma_{ee} = 276 \pm 50$ eV lies in between the earlier two values. The comparison between the new measurements and the earlier results is given in Table I. From theoretical arguments¹⁴ the ψ'' is believed to be a 3D_1 state of charmonium which is however mixed with the ψ' , the 2^3S_1 state. The relatively large Γ_{ee} value gives an estimate for this mixing angle of $20.3^\circ \pm 2.8^\circ$.

Charmed Meson Branching Ratios. A measurement of the number of events in a given D decay channel, together with a Monte Carlo calculation of the corresponding detection efficiency for the given detector and the luminosity calibration gives σB . To obtain B, the branching ratio, the following properties of the ψ'' are assumed:

- The ψ'' is a state of definite isospin (0 or 1); this allows a prediction of the D^0/D^+ production ratio, namely $\sigma(D^0)/\sigma(D^+) \simeq p_0^3/p_+^3$ as expected for p-wave production. This reflects the difference between the D^0 and

Table I. Measurements of the $\psi(3770)$ Resonance Parameters.

Experiment	Mass MeV/c ²	Γ_{tot} MeV	Γ_{ee} eV	ΔM^* MeV/c ²
DELCO ¹¹	3770 ± 6	24 ± 5	180 ± 60	86 ± 2
LGW ¹⁰	3772 ± 6	28 ± 5	345 ± 85	88 ± 3
Mark II	3764 ± 5	24 ± 5	276 ± 50	80 ± 2

* ΔM is the mass difference between the $\psi(3684)$ and $\psi(3770)$.

D^+ masses (1863.3 MeV and 1868 MeV respectively).

• The ψ'' decays nearly entirely into $D\bar{D}$ (~ 99%). This is based on the $\Gamma_{\text{tot}}(\psi')$ to $\Gamma_{\text{tot}}(\psi'')$ ratio (~ 1/100); i.e., that the OZI-suppressed portion of the ψ'' decay width is of the same magnitude as the $\Gamma(\psi')$. These assumptions were checked for those events decaying into $D\bar{D}$ mesons which were both identified.

Another feature of the fact that the ψ'' decays into a pair of $D\bar{D}$ mesons is that in addition to the invariant mass of a given state one can also use the beam-energy-constrained mass

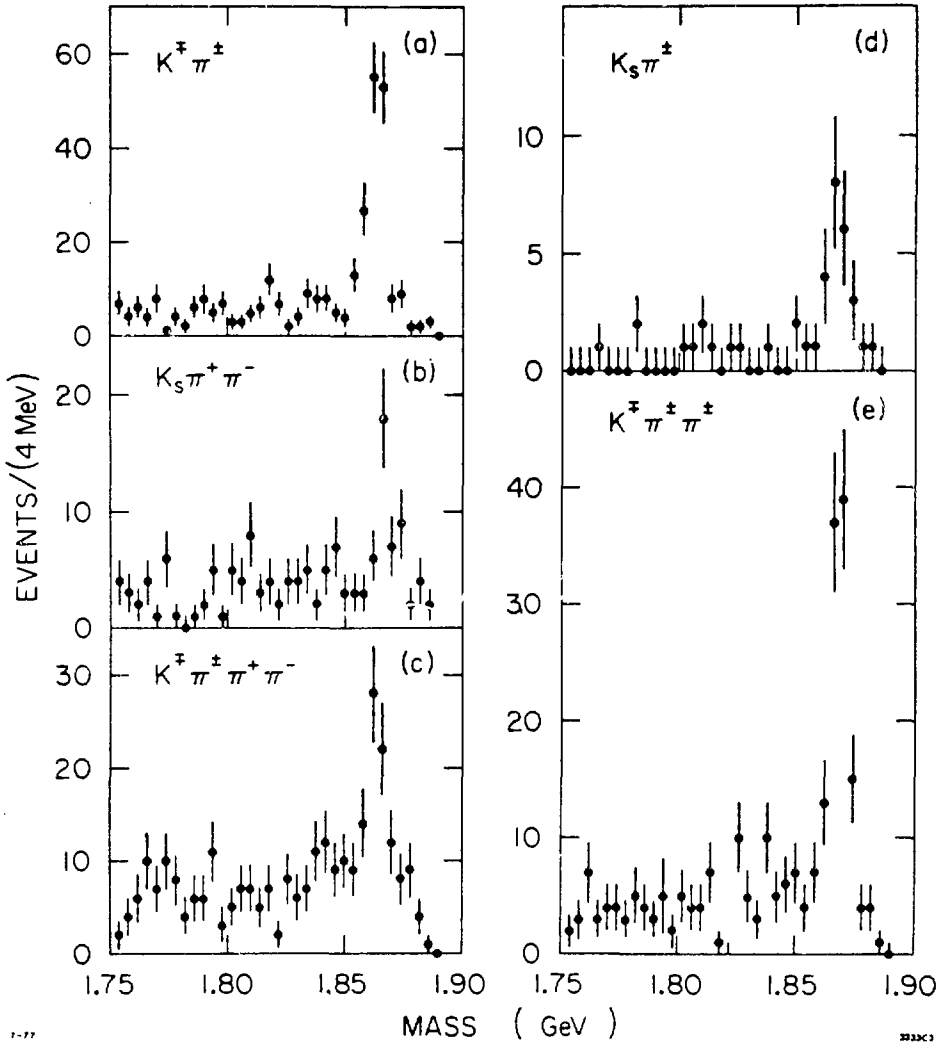
$$M_b = \sqrt{E_b^2 - p^2} .$$

This assumes that each particle combination which corresponds to a D decay mode has a total energy equal to the beam energy E_b . In practice particle combinations with energies within 50 MeV of E_b are accepted. Such a procedure results in marked reductions in background as well as much better mass resolutions (~ 3 MeV). Figure 11 shows the M_b distributions obtained for a number of D^0 and D^+ decay modes in the LGW experiment. In the data from the Mark II detector extensive running was carried out at $E_{\text{c.m.}} = 3.771$ GeV, an energy which lies slightly above the peak of the resonance mass, giving a total of 49,000 hadronic events. From the fit to the Breit-Wigner expression above, the $D\bar{D}$ pair cross sections at this energy is 6.85 ± 1.2 nb. When this value is apportioned between the D^0 and D^+ , this gives

$$\sigma_{D^0}(3.771) = 7.8 \pm 1.2 \text{ nb} \quad \text{and} \quad \sigma_{D^+}(3.771) = 5.9 \pm 1.0 \text{ nb}$$

for the two inclusive (single D) cross sections. Figures 12- 15 show the D^0 and D^+ decay modes obtained with the Mark II detector. Table II gives the hadronic branching ratios obtained in these two experiments.

• Cabibbo-Suppressed Decay Modes. An intrinsic feature of the GIM mechanism



XBL 7711-10397

Fig. 11. Beam-energy-constrained mass distribution from LGW experiment.

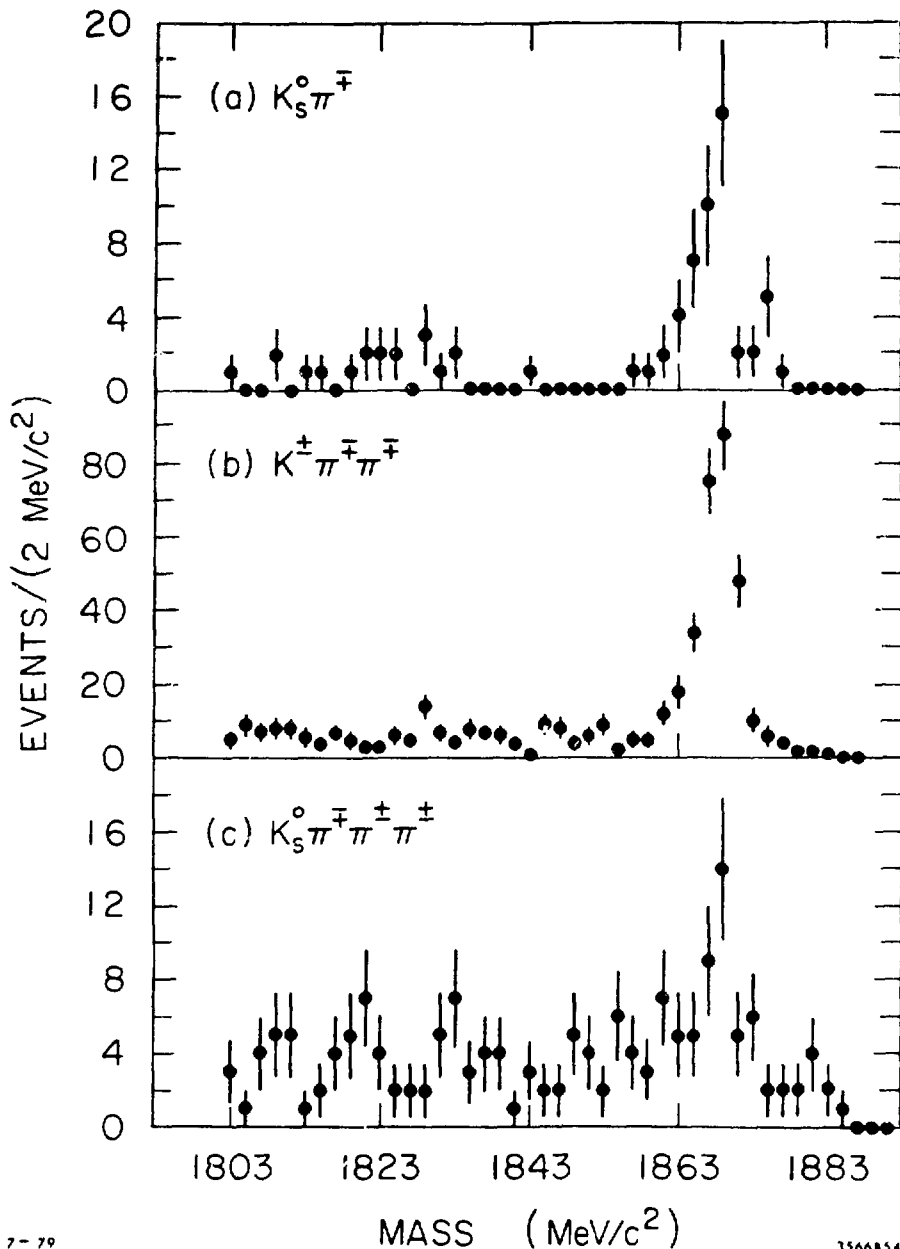


Fig. 12. Beam-energy-constrained mass distribution from the Mark II experiment with neutral D decays.

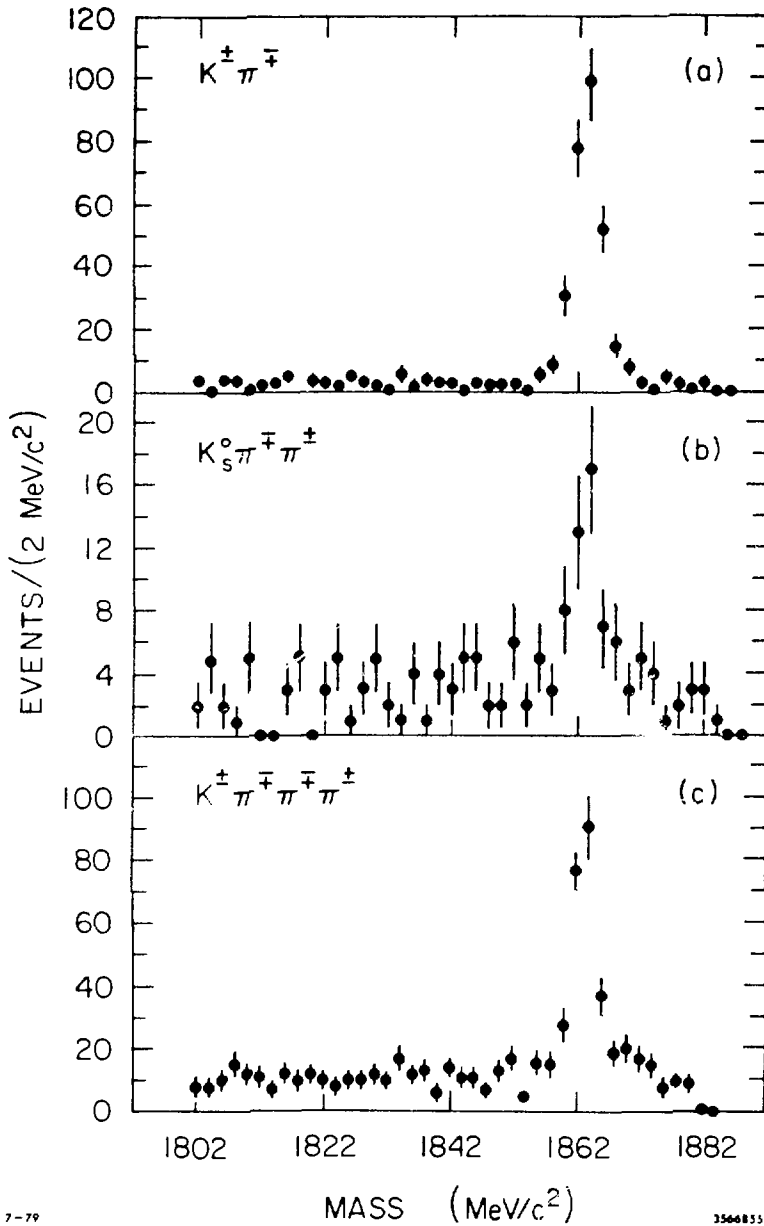


Fig. 13. Beam-energy-constrained mass distribution from the Mark II experiment with charged D decays.

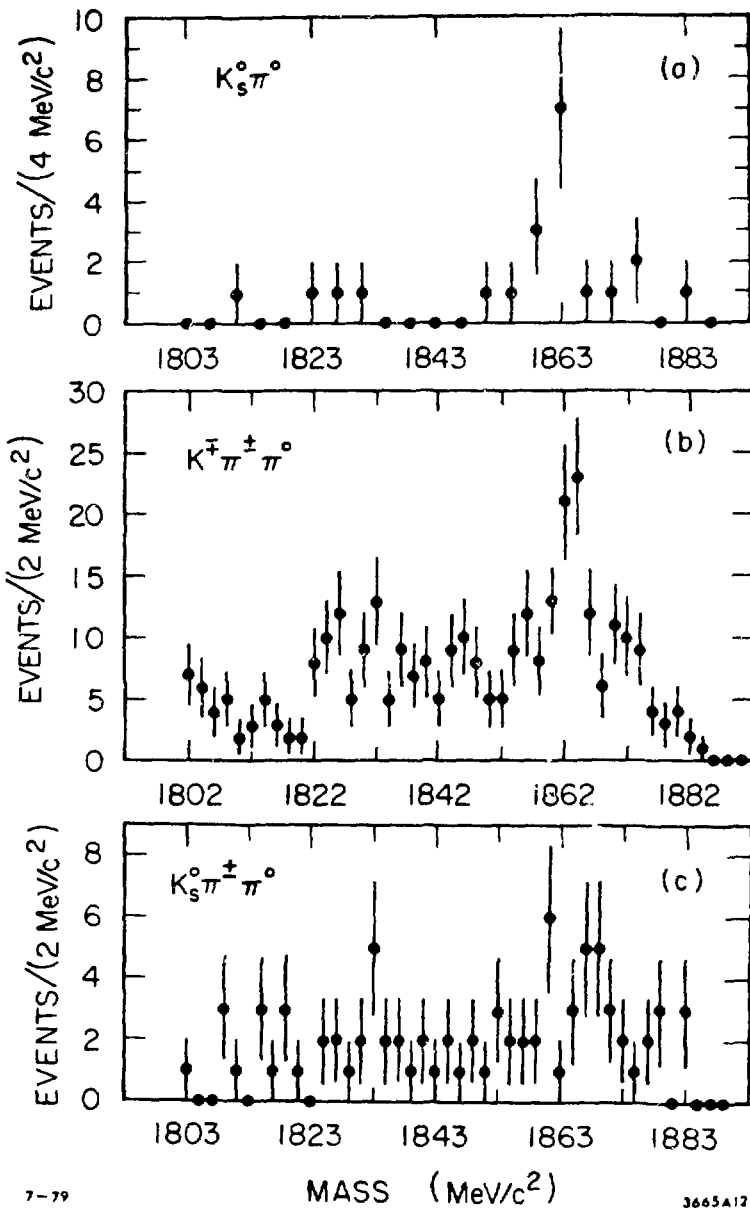
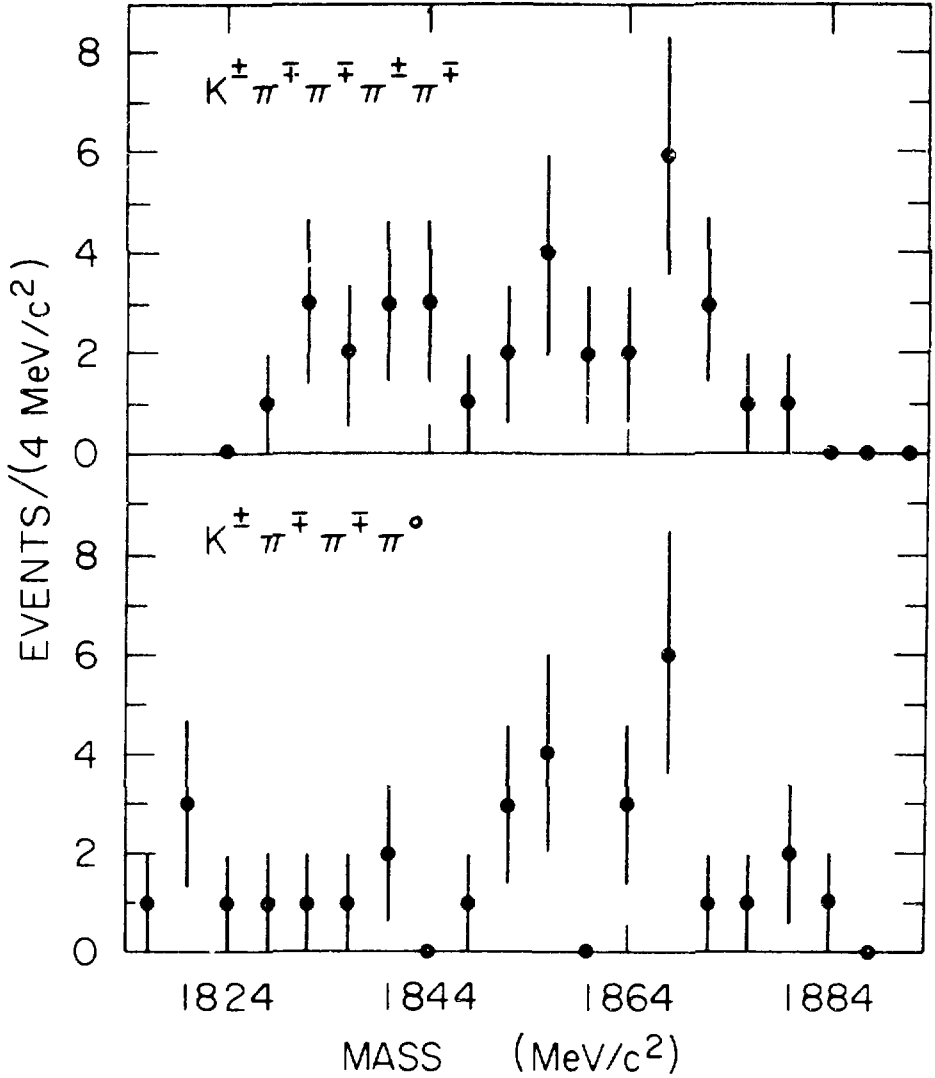


Fig. 14. Beam-energy-constrained mass distribution from the Mark II experiment with various D decays.



XBL 801-7874

Fig. 15. Charged D decays to $K^{\pm} \pi^{\mp} \pi^{\mp} \pi^{\pm} \pi^{\mp}$ and $K^{\pm} \pi^{\mp} \pi^{\mp} \pi^0$ (beam-constrained).

Table II, D-Meson Branching Ratios from the SLAC-LBL Mark II Detector and a Comparison with the LGW Experiment.

Mode	# Events	ϵ	BR (%)	LGW BR (%)
$\bar{D}^0 \pi^+$	271 ± 17	0.436	2.8 ± 0.5	2.2 ± 0.6
$\bar{K}^0 \pi^0$	9 ± 3	0.021	2.1 ± 0.6	
$\bar{K}^0 \pi^+ \pi^-$	39 ± 7	0.064	2.7 ± 0.7	4.0 ± 1.3
$K^- \pi^+ \pi^0$	37 ± 9	0.028	6.3 ± 2.2	12.0 ± 6.0
$K^- \pi^+ \pi^+ \pi^-$	197 ± 16	0.133	6.7 ± 1.4	3.2 ± 1.1
$\pi^+ \pi^-$	9 ± 4	0.50	0.2 ± 0.01	
$K^+ K^-$	22 ± 5	0.37	0.31 ± 0.09	
$\bar{K}^0 \pi^+$	37 ± 7	0.10	2.1 ± 0.5	1.5 ± 0.6
$K^- \pi^+ \pi^+$	251 ± 17	0.29	5.2 ± 1.0	3.9 ± 1.0
$\bar{K}^0 \pi^+ \pi^0$	9 ± 4	0.004	16.4 ± 9.5	
$\bar{K}^0 \pi^+ \pi^+ \pi^-$	22 ± 7	0.025	5.1 ± 2.0	
$K^- \pi^+ \pi^+ \pi^+ \pi^-$	5 ± 3.5	0.041	$< 2.0^*$	
$\bar{K}^0 K^+$	6 ± 3	0.07	0.5 ± 0.27	

* 90% confidence limit.

for charm is the prediction that aside from the principal (Cabibbo-favored) D decay modes, which lead to K^- or \bar{K}^0 in the final states, there also be the Cabibbo-suppressed modes leading to zero strangeness final states. The Cabibbo-favored and -suppressed modes for D^0 two-particle final states are illustrated by the quark diagrams in Fig. 16. Here the angle θ_A is the familiar Cabibbo angle θ_C while θ_B is the new angle which in the four-quark model is associated with the flavor mixing of charmed quarks. The GIM assumption is that $\theta_A = \theta_B$. Experimentally the two angles can be independently measured as:

$$\tan^2 \theta_A = \frac{\Gamma(D^0 \rightarrow K^- K^+)}{\Gamma(D^0 \rightarrow K^- \pi^+)} \quad \text{and} \quad \tan^2 \theta_B = \frac{\Gamma(D^0 \rightarrow \pi^- \pi^+)}{\Gamma(D^0 \rightarrow K^- \pi^+)} .$$

Figure 17 shows the experimental result from the Mark II experiment. Here the $\pi^- \pi^+$, $K^- \pi^+$ and $K^- K^+$ invariant masses are shown for two-particle combinations with momenta within 30 MeV/c of the expected D pair momentum of 288 MeV/c for $E_{c.m.} = 3.771$ GeV. Aside from the signals in the three channels at the D mass one notes kinematic reflections shifted by about ± 120 MeV/c²

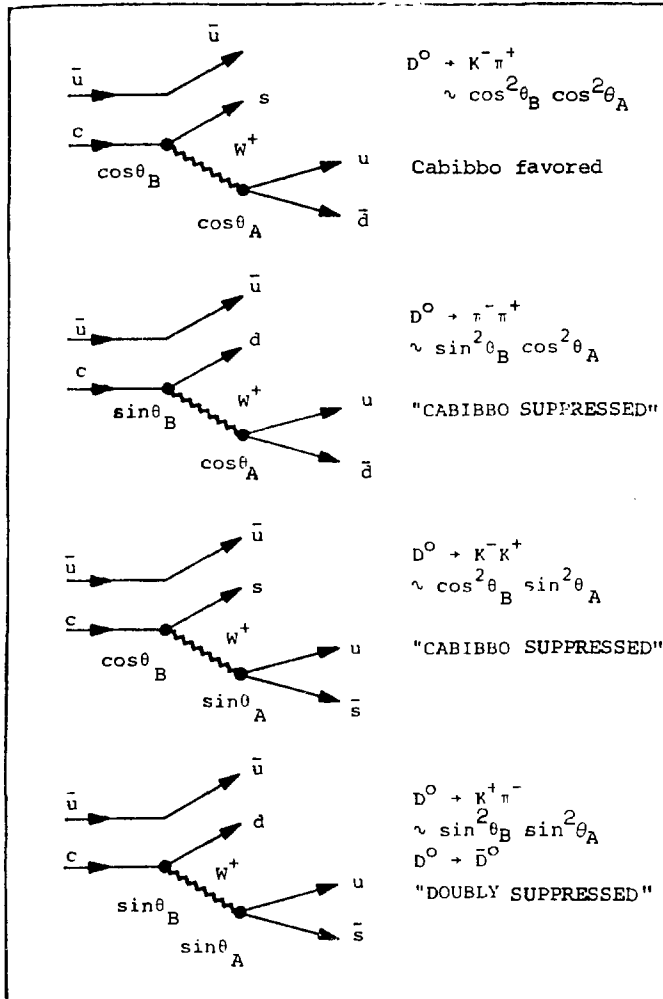
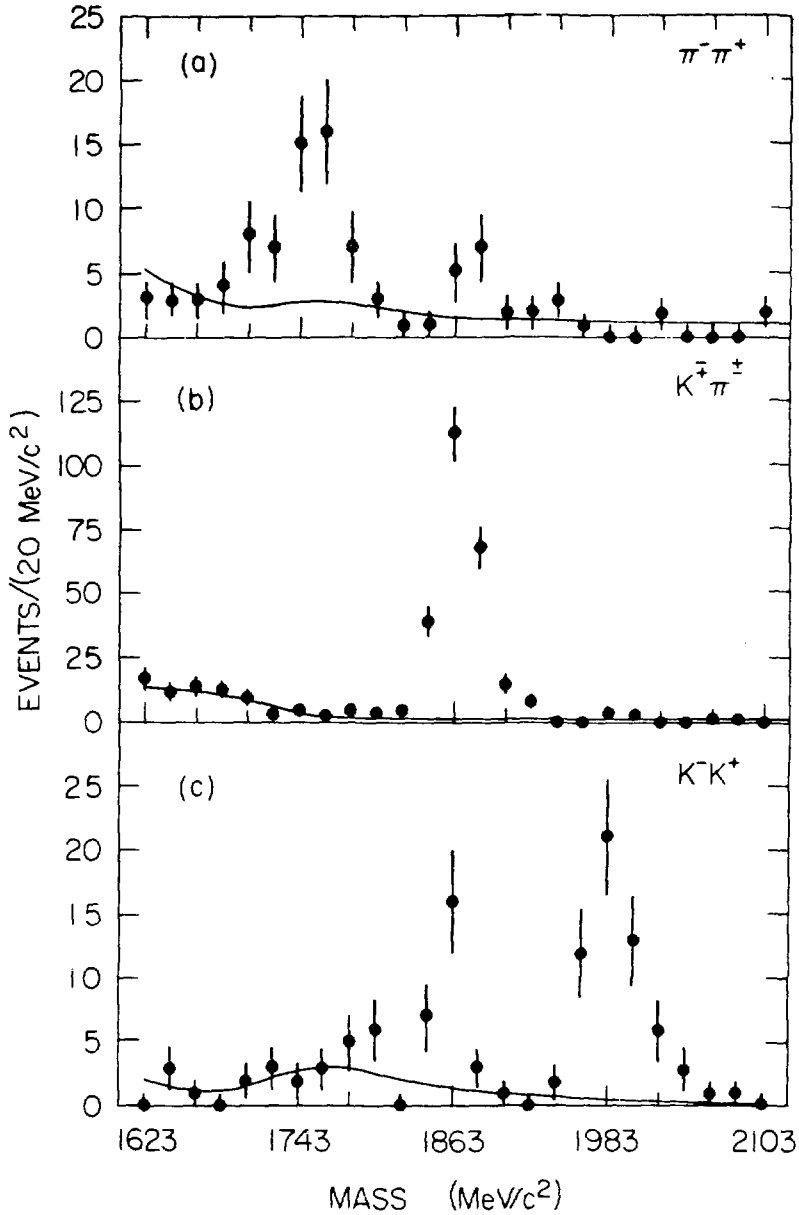


Fig. 16. Quark diagrams for D^0 decays.



XBL 801-7873

Fig. 17. Projections onto the invariant mass axes for $\Delta P_D = \pm 30$ MeV/c. Curves are fitted background from sidebands_D in ΔP_D .

from the D mass due to $\pi \leftrightarrow K$ misidentifications. A fit to the data yields $235 \pm 16 K^{\mp} \pi^{\pm}$ events, $22 \pm 5 K^+ K^-$ events and $9 \pm 3.9 \pi^+ \pi^-$ events.¹⁵ Accounting for the relative K and π detection efficiencies give

$$\frac{\Gamma(D^0 \rightarrow K^- K^+)}{\Gamma(D^0 \rightarrow K^- \pi^+)} = 0.113 \pm 0.03$$

and

$$\frac{\Gamma(D^0 \rightarrow \pi^- \pi^+)}{\Gamma(D^0 \rightarrow K^- \pi^+)} = 0.033 \pm 0.015 .$$

Here the quoted errors include systematic effects. The results clearly demonstrate the existence of the Cabibbo-suppressed decay modes of roughly the expected magnitude: $\tan^2 \theta_C \simeq 0.05$.

(3) D Meson Lifetime Ratios

Work at the ψ also allows the study of "tagged" events. This method has been used in LGW experiment and more recently by the Mark II experiment. Here I will quote the recent Mark II results for nearly 300 D^+ and 500 D^0 tagged events. In "tagging" we assume that at the ψ if a D^+ (D^0) is observed the remaining tracks in the event correspond to D^- (\bar{D}^0) decay. Hence for electron identification we can distinguish "right sign e" and "wrong sign e." The results are shown in Table III. After background subtraction and allowance for "wrong sign e" contributions we find a larger $B(D^+ \rightarrow e^+ + \dots)$

Table III. Semileptonic Decays of D^+ and D^0 .

Decay Mode	# Tags	# Electrons	Background	BR (%)
$D^+ \rightarrow e^+$	295 ± 18	38	15 ± 1	15.8 ± 5.3
$\rightarrow e^-$		4	3.9 ± 0.5	
$D^0 \rightarrow e^+$	480 ± 23	36	19 ± 1	5.2 ± 3.3
$\rightarrow e^-$		19	12 ± 1	

than $B(D^0 \rightarrow e^+ + \dots)$. On the theoretical assumption that $\Gamma(D^+ \rightarrow e^+ + \dots) = \Gamma(D^0 \rightarrow e^+ + \dots)$ we thus obtain:

$$\frac{\Gamma(D^0 \rightarrow \text{all})}{\Gamma(D^+ \rightarrow \text{all})} = \frac{B(D^+ \rightarrow e^+ + \dots)}{B(D^0 \rightarrow e^+ + \dots)} = \frac{\tau(D^+)}{\tau(D^0)} .$$

Hence from a maximum likelihood fit we obtain

$$\tau(D^+)/\tau(D^0) = 3.1_{-1.3}^{+4.1},$$

which is evidence for a larger D^+ than D^0 lifetime. A similar independent conclusion has been reached by the DELCO experiment.¹⁶ After corrections for phase space effects these measurements give a weighted average value of $B(D \rightarrow e^+) = (9.8 \pm 3.0)\%$.

Acknowledgment

I want to thank Mrs. C. Frank-Dieterle for her help and meticulous care in preparing and compiling this manuscript.

This work was supported primarily by the U. S. Department of Energy under Contract No. W-7405-ENG-48.

References

1. G. S. Abrams et al., Phys. Rev. Lett. 43, 477 (1979); 43, 481 (1979); 43, 1555 (1979); and 44, 10 (1980).
W. Davies-White et al., Nucl. Instrum. Methods 160, 227 (1979).
G. S. Abrams et al., to be published in IEEE Trans. on Nucl. Sci. NS-27, 1 (Feb. 1980); and NS-25, 1, 309 (1978).
Members of the SLAC-LBL Mark II collaboration are: G. S. Abrams, M. S. Alam, C. A. Blocker, A. M. Boyarski, M. Breidenbach, C. H. Broll, D. L. Burke, W. C. Carithers, W. Chinowsky, M. W. Coles, S. Cooper, B. Couchman, W. E. Dieterle, J. B. Dillon, J. Dorenbosch, J. M. Dorfan, M. W. Eaton, G. J. Feldman, H. G. Fischer, M. E. B. Franklin, G. Gidal, G. Goldhaber, G. Hanson, K. G. Hayes, T. Himel, D. G. Hitlin, R. J. Hollebeek, W. R. Innes, J. A. Jaros, P. Jenni, A. D. Johnson, J. A. Kadyk, A. J. Lankford, R. R. Larsen, D. Lüke, V. Lüth, J. F. Martin, R. E. Millikan, M. E. Nelson, C. Y. Pang, J. F. Patrick, M. L. Perl, B. Richter, J. J. Russell, D. L. Scharre, R. H. Schindler, R. F. Schwitters, S. R. Shannon, J. L. Siegrist, J. Strait, H. Taureg, V. I. Telnov, M. Tonutti, G. H. Trilling, E. N. Vella, R. A. Vidal, I. Videau, J. M. Weiss, and H. Zacccone.
2. A. De Rujula, H. Georgi, and S. L. Glashow, Phys. Rev. D12, 147 (1975) and M. K. Gaillard, B. W. Lee, and J. L. Rosner, Rev. Mod. Phys. 47, 277 (1975).
3. E. G. Cazzoli et al., Phys. Rev. Lett. 34, 1125 (1975); A. M. Cnops et al., Phys. Rev. Lett. 42, 197 (1979); C. Baltay et al., Phys. Rev. Lett. 42, 1721 (1979); C. Angelini et al., CERN Report No. CERN-EP 79-44, 1979 (to be published).

4. B. Knapp et al., Phys. Rev. Lett. 37, 882 (1976).
5. D. Drijard et al., Phys. Lett. 85B, 452 (1979); K. L. Giboni et al., Phys. Lett. 85B, 437 (1979); W. Lockman et al., Phys. Lett. 85B, 443 (1979).
6. M. Piccolo et al., Phys. Rev. Lett. 39, 1503 (1977).
7. R. Brandelik et al., Nucl. Phys. B148, 189 (1979).
8. This value is slightly model dependent. The quoted value was estimated from our measurement of $\Delta R(\Lambda + \bar{\Lambda})$ and $\Delta R(p + \bar{p})$ and a simple isospin statistical model.
9. G. Goldhaber et al., Phys. Rev. Lett. 37, 255 (1976); I. Peruzzi et al., Phys. Rev. Lett. 37, 569 (1976).
10. P. A. Rapidis et al., Phys. Rev. Lett. 39, 526 (1977).
11. W. Bacino et al., Phys. Rev. Lett. 40, 671 (1978).
12. A. Barbaro-Galtieri in Advances in Particle Physics, Vol. 2, R. Cool and R. Marshak, Editors, p. 193 (1968).
13. I. Peruzzi et al., Phys. Rev. Lett. 39, 1301 (1977).
14. E. Eichten et al., Phys. Rev. D17, 3090 (1978); T. Appelquist et al., Ann. Rev. Nucl. Sci. 29, 387 (1978).
15. G. S. Abrams et al., Phys. Rev. Lett. 43, 481 (1979).
16. J. Kirkby, 1979 International Symposium on Lepton and Photon Interactions at High Energy, Batavia, Illinois, August 23-29, 1979; SLAC-PUB-2419.